SPH SIMULATION OF HYDRODYNAMICS PROBLEMS RELATED TO DAM SAFETY

Daria Gatti[(2)], Andrea Maffio[(1)], David Zuccalà[(2)], Antonio Di Monaco[(3)]

[(1)]Corresponding Author, CESI RICERCA SpA, Via Rubattino 54, 20134 Milano, Italy,
phone: +39 02 39925184; fax: +39 02 39924608; e-mail: andrea.maffio@cesiricerca.it
[(2)]CESI Centro Elettrotecnico Sperimentale Italiano Giacinto Motta SpA, Via Rubattino 54, 20134 Milano, Italy,
phone: +39 02 21255180; fax: +39 02 21254678; e-mail: dgatti@cesi.it
[(3)]Consultant

ABSTRACT

Reservoirs and dams of hydropower schemes may give rise to safety hazards for population and infrastructures where scheme is located, in the presence of particular hydrogeologic circumstances, equipment malfunctioning and/or structural failure. Spillway insufficiency to discharge extreme floods, clogging of dam bottom outlets due to sedimentation, onset of landslide-induced waves in the reservoir, dam-break waves formation due to hypothetical dam collapse are example of issues encountered. Numerical modeling provides a useful tool to make predictive simulations of the hydrodynamics problems associated with the above issues, to assess hydraulic variables of interest e.g. flow pattern, propagation time and water height. In this paper numerical modeling based on SPH technique (*Smoothed Particle Hydrodynamics*) is applied to simulate unsteady and steady hydrodynamics of 2-D and 3-D test cases schematizing: dam-break flow with either water or *non-Newtonian* fluid (mud), landslide-induced waves coupled with landslide propagation in a reservoir (rigid block and granular material landslide), hydraulic jump formation downstream a dam spillway. SPH results for the 2-D test cases are compared to experimental data from laboratory physical models.

Keywords: SPH, dams, landslides, spillways, reservoir, impulse waves

1 INTRODUCTION

The presence of large mass of water in reservoirs impounded by dams in hydropower schemes, in conjunction with particular hydrogeologic circumstances (e.g. flood events, slope instability, etc.), equipment malfunctioning and/or structural failure, may cause hazards for population and infrastructures of the territory where scheme is located (ICOLD, 2003; ICOLD, 1989). Spillway insufficiency to discharge extreme floods, gate malfunctioning, clogging of bottom outlets due to sedimentation, may cause dam outlet works to fail releasing water to keep reservoir elevation below permitted maximum values. Slope instability and heavy precipitation may trigger significant volumes of land to slide into the reservoir; consequent water waves may run up and overtop the dam causing potential dam failure (particularly for earth dams) and possible flooding of the downstream valley. Besides, dam-break waves formation due to hypothetical dam collapse and/or breach formation have to be accounted for to assess inundation areas downstream of dam and to set up emergency plans for civil protection. Predictions via modeling (either physical or numerical) simulations of the hydrodynamic process associated with the above issues may be effective to support decision makers involved in managing, evaluating and mitigating hazards (dam owners, regulatory agencies, designers, etc.). In particular, tools based on numerical simulations are nowadays promising also considering the steadily increasing computer power and graphic capabilities.

Different numerical approaches and solution algorithms can be adopted to numerically model the hydrodynamic problems encountered in reservoir and dam safety depending on the study purpose, data available, user expertise, problem space/time scales of interest.

Schematizations based on shallow-water equations (either 1-D or 2-D approximation), and on *RANS-Reynolds Averaged Navier-Stokes* equations (3-D approximation with turbulence models in *CFD-Computational Fluid Dynamics* approach) are examples of modeling technique currently used in engineering practice (e.g. Olsen, 2000, Higgs, 1997).

An alternative innovative modeling approach known as *Smoothed Particle Hydrodynamics* (*SPH* in the following), originally developed for astrophysical problems, has been gaining increasing interest from the scientific community and application to a variety of fluid-dynamics problems (Monaghan, 1994; Gallati, 2006). SPH has no need of a computational grid (so-called *meshless* approach), whereas *fixed-grid* either shallow-water or *RANS* equations approaches need creating finite-difference/volume/element meshes. Also, *SPH* formulation allows for built-in capabilities permitting to deal with different fluid phases (e.g. liquid-solid-air) and to simulate strongly transient flows in complex geometries, without the difficulties often encountered in detecting a free-surface with *fixed-grid* approaches.

Hydrodynamics problems of interest in reservoir and dam safety exhibit flow features (e.g. strong free surface curvatures in spillway flow, air-water mixture formation in hydraulic jump, solid-water coupling dynamics in landslide-induced waves) are well suited to be advantageously simulated with *SPH* approach. Hence, within the framework of R&D activities of CESI RICERCA and aimed at improving the Italian electric system, two research projects about *SPH* development and application to hydrodynamics related to reservoirs and dam safety were set up in 2004 (Gatti, 2005) and 2006 (Maffio, 2006), respectively.

In the framework of this research activity, a three-dimensional code named SPHERA was developed. As the required computer time may be significant in simulation of real complex cases, development of a parallel new version of SPHERA is also in progress (Guandalini, 2006). In this paper a review of the research activity carried out so far and in progress is presented. Firstly, the hydrodynamic problems related to reservoir and dam safety simulated with SPH are shown. Secondly, SPH formulation in terms of governing equation, solution algorithms and boundary conditions is reported. Finally, main results obtained from the numerical simulations are discussed.

2 HYDRODYNAMICS PROBLEMS AND TEST CASES CONSIDERED

Hydrodynamics test cases considered for SPH simulation in this paper are simple schematizations of flows encountered in actual applications. Test cases are designed to highlight single flow features in order to better evaluate modeling response, limit computational burden, and make comparisons to available data from two-dimensional laboratory flumes.

Firstly, dam-break flows test cases are considered with either water or mud. In the latter case, a non-Newtonian fluid with given material rheology parameters is modeled via different specific relationship for the shear stress term in the governing equations (Komatina, 2004). Secondly, landslide propagation and induced waves in a flume are presented (Fritz, 2002). Landslide and waves are schematized as two dynamically coupled fluids. The landslide solid nature is modeled as either non-Newtonian or granular flow depending on type and fraction of solid present. Finally, a classical hydraulic jump either on a horizontal plane or with a positive/negative step is considered as a first approximation test case to evaluate flow in a stilling basin downstream a spillway (Hager, 1990). Numerical simulation SPH results are compared to experimental data for 2-D test cases. To evaluate SPHERA capabilities to deal with more complex flows, two examples of 3-D dam-break flows are also considered.

3 SPH FORMULATION

Introduced at the end of the seventies by Lucy (1977) and Gingold and Monaghan (1977), SPH has been applied to a wide range of physical and geometrical configurations, e.g.

Benson (2001), Shapiro (1996), Morris (1997), Cleary (1999). Later the method was reformulated to simulate hydrodynamics phenomena and free surface flows (Monaghan, 1992 and 1994).

In the SPH technique a fluid (or solid) body is represented by means of a discrete set of particles with physical properties (density, pressure, velocity, energy, temperature, etc.) distributed within a finite volume Ω, called *domain of influence* of the particle, according to a continuous and regular function W called *kernel*. To preserve symmetry, the shape of the domain of influence is a circle in two dimensions and a sphere in three dimensions. The kernel is defined as a symmetric function around the particle centre that vanishes outside the influence domain: the radius of this domain is $2h$ where h is the so called *smoothing length* representing the discretization scale.

Hence, in SPH any scalar or vectorial physical entity f (function of space) is approximated in any point $P_i(\mathbf{x}_i)$ by means of the summation

$$< f(\mathbf{x}_i) > = \sum_{j=1}^{N_i} f_j \, W\left(\left|\mathbf{x}_j - \mathbf{x}_i\right|, h\right) \Delta V_j \tag{1}$$

where $<f(\mathbf{x}_i)>$ represents the approximation of $f(\mathbf{x}_i)$, N_i the number of particles P_j in the neighbourhood of point $\mathbf{x}_i$ (i. e. such that the distance $|\mathbf{x}_j-\mathbf{x}_i|<2h$), f_j the function value in the centre of particle P_j, ΔV_j the volume element associated to particle P_j.

Approximation of spatial derivatives of function $f(\mathbf{x})$ and differential operators like gradient and divergence (for vectorial functions) can be drawn from summation (1), in accordance with the derivability and normalization properties of the kernel W

It can be shown (Monaghan 1992) that mass and momentum balance Navier-Stokes equations for compressible viscous fluids in the lagrangian form can be approximated as:

$$\frac{d\rho}{dt} = -\rho \, div \, \mathbf{v} \tag{2}$$

$$\frac{d\mathbf{v}}{dt} = -\frac{1}{\rho}\mathbf{grad}\, p + \nu \, div \, \mathbf{grad}\, \mathbf{v} \tag{3}$$

With reference to the centre of the generic particle P_i, these equations can be respectively discretised into (4) and (5), plus the kinematic equation (6):

$$\frac{d\rho_i}{dt} = -\sum_{j=1}^{N_i} m_j \left(\mathbf{v}_j - \mathbf{v}_i\right) \cdot \mathbf{grad}_i \, W\left(r_{ij}, h\right) \tag{4}$$

$$\frac{d\mathbf{v}_i}{dt} = -\sum_{j=1}^{N_i} m_j \frac{p_i + p_j}{\rho_i \rho_j} \mathbf{grad}_i \, W\left(r_{ij}, h\right) - 2\nu \sum_{j=1}^{N_i} \frac{m_j}{\rho_i r_{ij}} \left(\mathbf{v}_j - \mathbf{v}_i\right) \left(\frac{\partial W}{\partial r}\right)_j . \tag{5}$$

$$d\mathbf{x}_i / dt = \mathbf{v}_i \tag{6}$$

where ρ_i, p_i and $\mathbf{v}_i$ are density, pressure and velocity of the generic particle $°P_i°$; N_i is the number of particles $°P_j°$ interacting with particle $°P_i°$; $r_{ij}=|\mathbf{x}_j-\mathbf{x}_i|$ is the distance between particles $°P_i°$ and $°P_j°$; ν is the kinematic viscosity of the fluid.

Finally the state equation of the generic particle is needed:

$$p_i = p_0 + c_0^2 \left(\rho_i - \rho_0\right) \tag{7}$$

(ρ_0 and p_0 are reference values of density and pressure, c_0 is the celerity of perturbations).

In problems with fluid flows in confined domains (as encountered in the applications considered in this work), it is necessary to take into account the interactions between fluid particles and solid boundary (either terrain or structures). Several methods have been proposed in literature to impose boundary conditions (Monaghan, 1992), e.g. the *ghost particle* and the *fixed particle* methods. However, either method may not be adequate to simulate efficiently engineering applications with complex boundaries and three-dimensional geometry. Hence, an alternative method which applies to irregular boundaries represented by polygonal straight lines and by polyhedral surfaces with plane triangular faces, in two and three dimensions, respectively, has been devised by the Authors. This technique is based on

the evaluation of the contributions of the boundary to the equations of the generic particle at a distance $<2h$ by means of integrals extended over the intersections of the domain of influence of particle $°P_i°$ with the line/face of the boundary. For example, the additional terms to account for boundaries in the mass balance equation of a particle P_i are:

$$\frac{d\rho_i}{dt} = -\sum_{j=1}^{N_i} m_j \left(\mathbf{v}_j - \mathbf{v}_i\right) \cdot \mathbf{grad}_i W\left(r_{ij}, h\right) - \rho_i v_{in} \left(\int_{S_b} W\left(r_Q, h\right) dS + \frac{1}{\eta_i} \int_{\Omega_b} W\left(r, h\right) d\Omega \right) \qquad (4')$$

where S_b the part in the solid due to the intersection of the boundary line/face with the circle/sphere of influence of particle P_i; Ω_b the part of Ω remaining outside the boundary; $r_Q=|\mathbf{x}_Q-\mathbf{x}_i|$ the distance between particle P_i and integration point $\mathbf{x}_Q$ on the line/face S_b; $r=|\mathbf{x'}-\mathbf{x}_i|$ the distance between particle P_i and integration point $\mathbf{x'}$ internal to the domain Ω_b; v_{in} the component of particle velocity normal to the side/face S_b; η_i distance of particle P_i from the side/face S_b. Similarly to eq. (4'), additional terms appear in the momentum equation. Integrals can be evaluated either analytically in particular cases or numerically.

The original system of partial differential equations (2), (3) is thus formulated into a system of $3N$ ordinary differential equations (4), (5), (6) plus N algebraic equations (7), being N the total number of particles. This system can be integrated numerically by means of explicit algorithms to obtain in a lagrangian framework the successive position of particles together with all the relevant physical entities. Particles can be initially grouped in several media with different physical and rheological properties to describe either *newtonian* or *non-newtonian* fluids such as water, mud or landslide material like debris, granular material etc.

In moving fluids internal stresses take place with normal and tangential components. Tangential components τ, opposite to the fluid movement, can be described with different relationships depending on the angular deformation velocity $\dot{\gamma}$ and other parameters in accordance with the fluid rheology behaviour. In *newtonian* fluids, for a given temperature, the relationship $\tau = \mu\, \dot{\gamma}$ holds, where μ is the fluid viscosity assumed as constant in Navier-Stokes equation (3). In *non-newtonian* fluids, equation (3) can be maintained formally unchanged provided the viscosity μ be treated not as a constant, but as a parameter varying in space and time inside the fluid volume, according with the rheology properties of the material, and evaluated in SPH for each particle and time instant. Assuming the general relation $\tau = \tau_c + K\, \dot{\gamma}^n$ (where K is called *consistency* and τ_c is the critical shear stress), an apparent viscosity defined as $\mu_{app} = \tau / \dot{\gamma} = K\, \dot{\gamma}^{n-1}$ can introduced in equation (3).

As shown in Fig. 1, the change of the exponent n results in rheological curve corresponding to different fluid behaviour. As often encountered in landslides, shear stress $\tau > \tau_c$ is needed to trigger fluid movement (Bingham and Herschel-Bulkley like fluids).

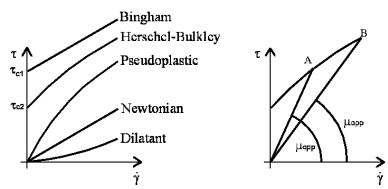

Fig. 1: Rheological curves

In the presence of landslides with high fraction of granular material (sand, gravel, fractured rock), surface forces are negligible and shear resistance is characterised by the friction angle φ. Considering the stress-strain relation in granular materials (Mohr-Coulomb criterium), a further relationship for the apparent viscosity can be used (depending on fluid pressure, angular deformation velocity, friction angle) leaving equation (3) formally unchanged.

4 THE SPHERA CODE

The SPHERA computer code (***S**moothed **P**article **H**ydrodynamics **E**valuation of **R**ockfall- and **A**valanches-generated waves*), has been developed in CESI RICERCA since 2004 to provide a software tool based on SPH technique for R&D and engineering

applications. Initially developed to simulate landslide-induced waves in reservoirs and landslide propagation in two and three dimensions, the code has been extended to other hydrodynamics problems related to dam safety e.g. flows downstream dam spillways.

From the computational point of view, SPHERA code implements an explicit *Staggered-Euler* (SE) algorithm for time integration of the ordinary differential equation system (4), (5), (6) which appears to be effective with respect to other explicit algorithms, though a Courant stability criterion limiting maximum time step has to be considered. Computational skills are also implemented to improve numerical stability and simulation accuracy: the artificial viscosity (Monaghan, 1992), particularly effective in problems with impacts and shocks; density and velocity smoothing procedure, to dump numerical fluctuations with wave length lower than the particle smoothing length; kernel re-normalization, to improve accuracy approximation of velocity spatial derivatives due to viscous stress in *non-newtonian* fluids or turbulence modeling. SPHERA code is written in *FORTRAN* language and includes a graphical interface for input data management and simulation results visualization.

A first parallel version of SPHERA code has also been developed, to limit computational cost when simulating complex flows in three-dimensional geometry encountered in engineering applications. The parallel version has been designed (e.g. high level of portability, no special licence requirements, etc.) to suit to users with no access to fast supercomputers and with no special skills for installation, as reported in Guandalini (2006).

5 SPH SIMULATIONS

5.1 DAM-BREAK AND MUD FLOW TESTS PROPAGATING ALONG A CHANNEL

In a first test SPHERA reproduces a water dam-break in a 1,2 m long laboratory flume (Gallati, 2000). A volume of water, released by quickly removing the gate, propagates over the initially dry channel bottom. The flume, equipped with a transparent wall, has been photographed at some instants after the water release, highlighting the typical dam-break wave profile. A 2D schematisation in the vertical plane and 4800 particles have been used for the SPH simulation. Fig. 2, where SPH results are superimposed upon the photographs, shows agreement between experiment and numerical data: water profiles, front propagation times and flow run-up at the end of the channel are fairly captured. Numerical results do not change appreciably if Monaghan and other numerical parameters vary in reasonable ranges.

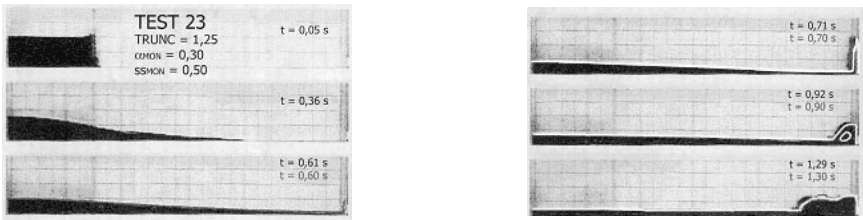

Fig. 2**:** Dam-break along a channel: photographed water (dark area) matches the simulated water profile (light track)

The second simulation is a water dam-break, schematised as 3D, in a horizontal channel with vertical walls. An obstacle is located on the right-hand side of the channel in order to trigger flow asymmetries. Solid walls (horizontal bottom, vertical walls and obstacle) are made up of fixed particles (numerically prevalent). The liquid flow is perfectly symmetric until the obstacle is encountered. After the impact the right side of the water front runs up along the obstacle wall (Fig. 3), whereas the left side continues to propagate along with a transverse velocity component. As a consequence, the impact with the wall at the end of the channel generates a fan-shaped run-up. Results are qualitatively persuasive, although there is no experimental counterpart available.

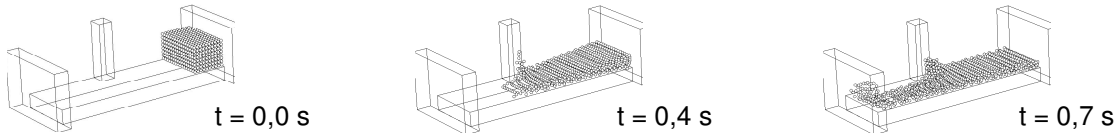

Fig. 3: 3D dam-break along a channel: some instants of the simulation

Next test case is related to a water dam-break over dry bed, along a valley with bends schematised as a 3D simplified though useful geometry. Numerical results appear qualitatively reasonable thus confirming the SPH technique ability to catch phenomena that are intrinsically 3D.

Fig. 4: Simplified dam-break 3D geometry (left: before dam-break; right: propagating wave)

Water run-up along terrain slopes at bends is also appreciated.

Another series of dam-break tests has been performed with many different non-Newtonian fluids (grains, Bingham, etc.). The example reproduced in Fig. 5 refers to a water-clay mixture propagating along a sloping (1%) channel; the SPH simulations has been prepared trying to reproduce Komatina experiments with a 4,5 m long laboratory flume (Komatina 2004). Fig. 5 illustrates the rheological charactertistics of the mixture, that exhibits a non zero critical shear stress, along with comparison between SPH results and experiment at three time instants (shaded area: SPH with mud simulated with about 12000 particles; dots: experimental data profiles). Simulations of highly viscous and/or non-newtonian fluids are more difficult than simulations with water (for example time steps considerably reduce and the output can be more sensible to parameter variations); however propagation times appears correctly reproduced. The nail-shaped front, due to adhesion to the channel bottom and qualitatively different from the case of water dam-break over a smooth bottom, should also be noted. Internal friction of the fluid makes useless artificial dissipation in the numerical model.

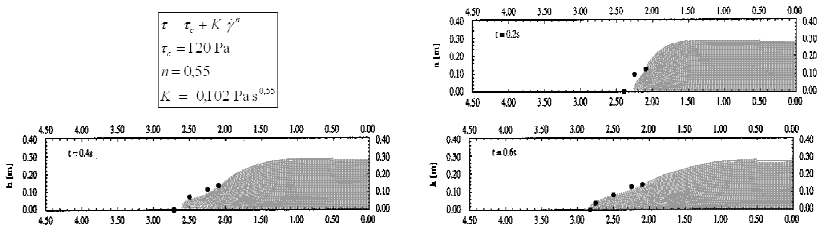

Fig. 5: Komatina mud dam-break experiment (dots) compared with SPH simulation (grey area)

5.2 LANDSLIDE-INDUCED WAVES IN A RESERVOIR

In the following test cases, dynamics of impulse water wave generation due to landslides is simulated. The Authors considered the experimental data collected in experiments at ETH-VAW laboratory in Zürich. The experimental setup (fully described in Fritz, 2002) includes a rectangular prismatic wave tank 11 m long, 0,5 m wide and 1 m deep. At the front of the tank a 3 m long, a hillslope ramp (angle 45°) was built. Many tests were performed, with a rigid block (Zweifel, 2007) and granular landslide (Fritz, 2002). A wood squared parallelepiped and polypropilene were used to schematized the rigid block and granular landslides, respectively. The granular slide was released by means of a pneumatic landslide generator with an integrated slide box controlling the impact slide velocity.

Fig. 6 shows the impulse wave generation with the rectangular block. The water profile due to the complex hydrodynamic phenomenology is well reproduced, so consequent impulse waves can be evaluated with the correct height.

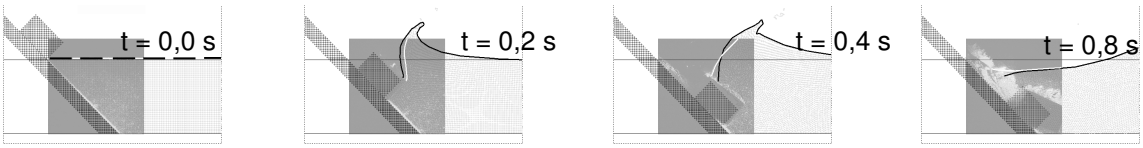

Fig. 6: Impulse waves generated by a rigid landslide: dark square: photographed area – white line: photographed water profile – black line: simulated water profile

Experiments with granular slides show distinct phenomena at impact site depending on the landslide velocity, due to differences in the process of energy and momentum exchange. The characteristic non-dimensional parameter is the *landslide Froude number* defined as $Fr=\upsilon/(gd)^{0,5}$ (υ = landslide velocity, g = gravity acceleration of gravity, d = water depth).

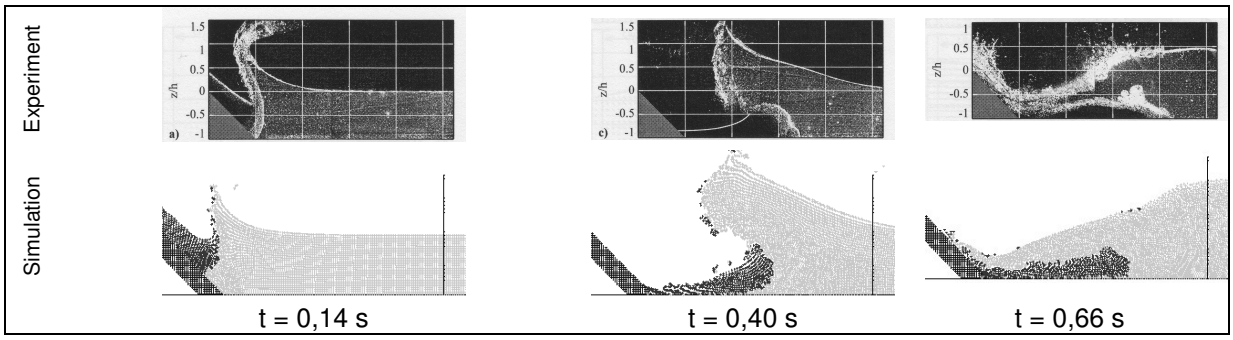

Fig. 7: Impulse wave generated by granular landslide, $2 < Fr < 3$

The above simulations along with other test cases simulated by the Authors and not reported here would confirm the SPH technique able to simulate rapidly varying complex multi-phase phenomena involving water, viscous *newtonian* fluids, *non-newtonian* fluids and granular landslides for the laboratory experiments considered. Extensive experiments show that if $Fr < 2$ there is continuity between landslide and water; if $2 < Fr < 3$, an air crater develops between landslide and water, then it collapses backwards; if $Fr > 3$, a forward collapsing air crater develops (Fritz, 2002). Fig. 7 and Fig. 8 compare experiments and simulations for the cases $2 < Fr < 3$ and $Fr > 3$. SPH simulations correctly reproduce all the significant characteristics of impact and wave generation, e.g. landslide and wave shape and propagation along the flume.

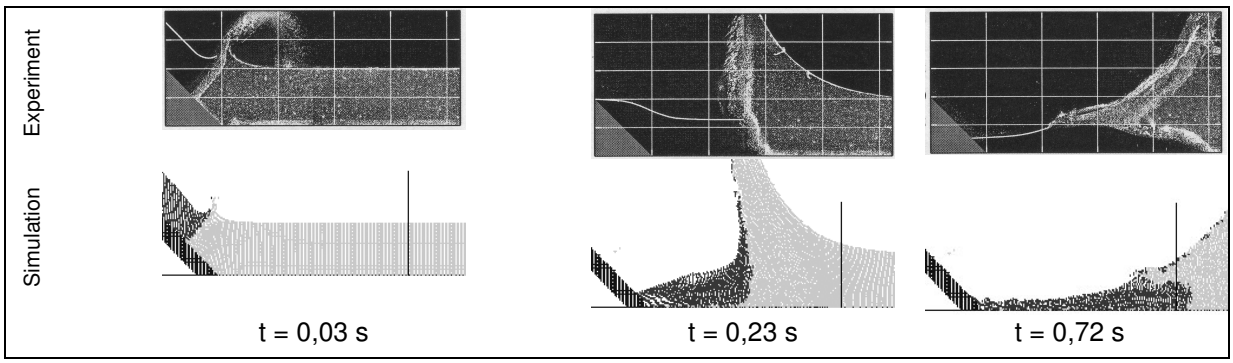

Fig. 8: Impulse waves generated by a granular landslide, $Fr > 3$

6 HYDRAULIC JUMP

A recent application in progress focuses on the simulation of free surface flow occurring in stilling basins located downstream of dam spillways, to dissipate the energy of the discharged water. Main dissipation mechanism takes place inside a hydraulic jump which have to remain steadily inside the stilling basin. Design of stilling basin is usually verified and optimized by means of a laboratory hydraulic model. The aim of the study in progress is to evaluate capabilities of SPH implemented in SPHERA code as a numerical tool to integrate

hydraulic laboratory studies. Preliminary application focuses on the hydraulic jump with different configurations proposed by Gallati (2006), a simplified though useful test to individuate and analyze critical simulation issues related to this type of flow. In particular three types of hydraulic jumps have been taken into consideration: (a) classical, (b) on positive step, (c) on negative step. A number of numerical simulation have been performed with reference to 2D hydraulic jumps for which experimental laboratory data are available.

As significant energy dissipation is expected inside the hydraulic jump, a turbulent viscosity ν_t is used in the simulation and imposed as either a constant value or a relation based on the mixing length concept as follows:

$$\nu_t = l^2\left(\frac{\partial u}{\partial y} + \frac{\partial v}{\partial x}\right) \tag{8}$$

where $l = \alpha h$ is the mixing length assumed constant and proportional to the smoothing length h (turbulent viscosity still varies in space in accordance with velocity spatial derivatives).

Fig. 9 (left) shows an example of a classic hydraulic jump (i.e. over a horizontal plane), with upstream depth h_1 = 0,02 m, upstream velocity u_1 = 1,94 m/s, upstream Froude number Fr_1 = 4,38, downstream depth h_2 = 0,12 m, downstream velocity u_2 = 1,32 m/s, downstream Froude number Fr_2 = 0,33. Imposed boundary conditions are upstream water depth and velocity, downstream velocity, though other types of boundary conditions have been also investigated. Free slip condition is applied at the bottom.

The main features of the jump were well reproduced, in particular the length of the roller L_r was consistent with the general experimental relationship found (Hager et al., 1990)

$$\frac{L_r}{h_1} = 8\left(Fr_1 - \frac{3}{2}\right) \tag{9}$$

giving a an experimental value of 0,46m to be compared to SPH result of 0,45m.

Jump toe position was sensitive to simulation parameters (e.g. tailwater depth), i.e. simulation small variation in parameters caused upstream/downstream displacement.

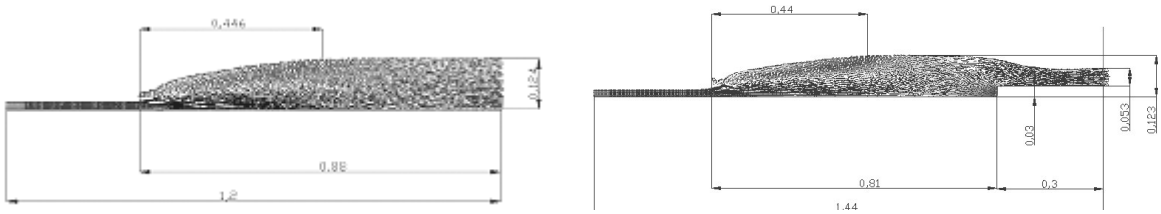

Fig. 9: Hydraulic jump simulations: classical (left) and on positive step (right)

Fig. 9 (right) shows the numerical simulation of a hydraulic jump on positive step, based on the experimental set up of University of Pavia (Gallati, 2003). Simulation data are: step height s = 0,03, downstream depth h_2 = 0,053 m (critical depth), velocity u_2 = 0,73 m/s (boundary condition), Froude number Fr_2 = 1,00 (other input data equal to classical jump). Free slip condition is applied at the bottom. Again, the main features of the jump were reproduced and agreement was found between SPH simulation and experimental data either from a qualitative and quantitative point of view (e.g. experimental roller length of 0,47m vs. SPH result of 0,44m). Finally, in Fig. 10 the SPH simulation of a hydraulic jump on negative step is shown. This reproduces one of the numerous laboratory experiments carried out by Kawagoshi and Hager (1990) aimed to characterize a particular type of jump known as *wave jump*, which takes place downstream of the negative step for a narrow range of values of the tailwater depth. This jump features a steady wave, just downstream of the bottom drop, with an underlying submerged vortex, and further downstream a steady surface roller. Simulation input data are: upstream depth h_1 = 0,0356 m, upstream velocity u_1 =1,891 m/s and Froude number Fr_1 =3.2 (boundary conditions), step height s = 0,077 m, downstream depth h_2 =

0,204 m (critical depth), downstream velocity u_2 =0,33 m/s (boundary condition), downstream Froude number Fr_2 = 0,233. Free slip condition is applied at the bottom. SPH simulation was able to reproduce qualitatively main features of the jump, e.g. the steady wave, the submerged vortex and the steady surface roller. With reference to the sketch in Fig. 10, an example of experimental data compared to SPH simulation results were: x_r=0,18m - l_r=0,76m - h_p=0,17m - h_w=0,25m (experimental) vs. x_r=0,16m - l_r=0,84m - h_p=0,17m - h_w=0,22m (SPH).

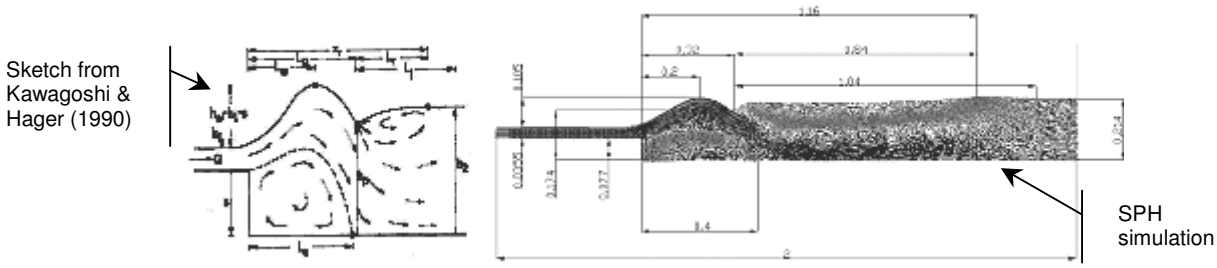

Fig. 10: Hydraulic jump on negative step

In all hydraulic jump simulations, type of downstream boundary condition and turbulent viscosity appeared to play a significant role. By using the turbulence model (mixing length), results were better reproduced and less sensitive to other dissipation parameters. Finally, better accurate results were obtained by imposing velocity at the downstream boundary rather than hydrostatic pressure profile or zero normal space derivatives.

7 CONCLUSION

For 2-D laboratory flumes test cases considered, quantitative fair agreement is obtained between experimental data and SPH simulation results. For 3-D test cases (designed to preliminary evaluate SPH capabilities with complex geometries), results appear qualitatively fair and worthwhile extending applications to more complex situations. Simulation tools based on SPH modeling are attractive for studying hydrodynamics problems related to safety, encountered in either design phase or operation of reservoir and dam. SPH capabilities to deal with multiphase, transient flows and free surface are potentially well suited to simulate hydrodynamics problems considered in this work, i.e. landslide-induced waves in reservoir, dam-break flow, hydraulic jump. Preliminary results obtained in the simulations presented in this paper are promising compared with available experiments. A new SPH modeling activity on sediment scour induced by dam bottom opening is in progress in collaboration with Pavia University – Italy. As research activity is aimed at developing software modeling tools to be used in engineering applications, emphasis is placed on evaluating SPH from the point of view of both accuracy and computational cost. Hence, work is also in progress to compare SPH results with others techniques (e.g. *CFD*). Future activities are expected to focus on more complex flow within a three-dimensional stilling basin downstream a dam spillway, and the upgrade of the parallel version of SPHERA code.

ACKNOWLEDGMENTS

Roberto Guandalini and Elia Bon (CESI RICERCA) who developed the first parallel release of SPHERA code, and Giordano Agate who contributed to SPH results processing, are gratefully acknowledged. Thanks are due to the Hydraulic Engineering Dept. of Pavia University – Italy for collaboration in developing the SPH model and helpful discussion. Finally, thanks are also due to ETH-VAW of Zurich – Switzerland for experimental data obtained in the frame of an agreement with CESI. This work has been financed by the Ministry of Economic Development with the Research Fund for the Italian Electrical System under the Contract Agreement established with the Ministry Decree of March 23, 2006.

REFERENCES

Benson, J. et al. (2001), A comparison of semi-analytic and smoothed particle hydrodynamics galaxy formation, *Mon. Not. R. Astron. Soc.* 320, 261-280.

Cleary, P. W., Monaghan, J. J. (1999), Conduction modelling using smoothed particle hydrodynamics, *J. Comput. Phys.* 148, 227.

Fritz, H. (2002), Initial phase of landslide generated impulse waves, *ETH-VAW (Swiss Laboratory of Hydraulics) publication n. 178*, Zürich.

Gallati, M. (2006), About SPH as an engineering tool: validation tests and open problems, *Invited Lecture, 1st SPHERIC Workshop*, Rome.

Gallati, M., Braschi, G. (2000), Simulazione lagrangiana di flussi con superficie libera in problemi di idraulica, *L'acqua,* 5/2000.

Gallati, M., Braschi, G. (2002), Numerical description of rapidly varied flows via SPH method, *IASTED Int. Conf.,* Crete, Greece, June 25-28, 2002.

Gallati, M., Braschi, G. (2003), Numerical simulation of the jump formation over a sill via SPH method, *Conf. on Modeling Fluid Flow (CMFF'03)*, Budapest, Sept. 3-6, 2003.

Gatti, D., Zuccalà,D., Bon,E. (2005), Validazione di un modello numerico basato sul metodo SPH per simulare la propagazione di corpi franosi, *Report CESI n. A5055706.*

Gingold, R. A., Monaghan, J. J. (1977), Smoothed Particle Hydrodynamics: theory and application to non-spherical stars, *Mon. Not. R. Astr. Soc.* 181, 375-389.

Guandalini, R. (2006), A parallelization approach of the 3D code SPHERA for the simulation of landslide-induced impulse waves in a reservoir, *1st SPHERIC Workshop*, Rome.

Hager, W.H., Bretz, N.V. (1986), Hydraulic jumps at positive and negative steps, *J. of Hydraulic Research*, 24 (4). 237-253.

Hager, W.H., Bremen, R., Kawagoshi, N. (1990), Classical hydraulic jump: length of the roller, *J. of Hydraulic Research*, 28 (5), 591-608.

Higgs, J.A. (1997), Folsom dam spillway vortices computational fluid dynamics model study, *Memorandum Report*, Bureau of Reclamation

ICOLD (2003), Dams and floods - Guidelines and case histories, *Bulletin 125*.

ICOLD (1989), Sedimentation control of reservoir, *Bulletin 67*.

Kawagoshi, N., Hager, W.H. (1990), Wave type flow at abrupt drops, *J. of Hydraulic Research*, 28 (2), 235-252.

Komatina, D., Dordevic, D. (2004), Numerical simulation of hyper-concentrated flows, *River Flow 2004,* ISBN 90 5809 658 0.

Lucy, L. B. (1977), A numerical approach to the testing of the fission hypothesis, *Astron. Journ.*, 82, 1013-1020.

Maffio A. (2006), Ongoing developments at CESI RICERCA, Milan, *SPHERIC Newsletter Issue* 3, Dec. 2006 (http://cfd.me.umist.ac.uk/sph/newsletters.html).

Monaghan, J.J. (1992), Smoothed Particle Hydrodynamics, *Annu. Rev. Astron. Astroph.* 30, 543-574.

Monhagan, J.J. (1994), Simulating free surface flow with SPH, *J. Comp. Phys.* 110, 399-406.

Monaghan, J. J., Price, D. J. (2001), Variational principles for relativistic smoothed particle hydrodynamics. *Mon. Not. R. Astron. Soc.* 328, 381-392.

Morris, J. P., Fox, P. J., Zhu, Y. (1997), Modeling low Reynolds number incompressible flows using SPH, *J. Comput. Phys.* 136, 214.

Olsen, N.R. (2000), CFD algorithms for hydraulics engineering, *Class notes Dept. of hydraulic and environmental engineering*, The Norwegian Univ. of Science and Tech.

Shapiro, P., Martel, H. , Villumsen, J., Owen, J. (1996), Adaptive SPH with application to cosmology, *The Astrophysical Journal Supplement Series*, 103, 269-330

Zweifel A., Zuccalà D., Gatti D. (2007), Comparison between computed ad experimentally generated impulse waves, *Journal of Hydraulic Engineering ASCE*, February 2007